Design and performance of multiloop and washer SQUIDs intended for sub-kelvin operation

Mikko Kiviranta†, Jari S Penttilä, Leif Grönberg, Juha Hassel, Antti Virtanen and Heikki Seppä

VTT Information Technology, Tietotie 3, FIN-02150 Espoo, Finland

Abstract. We have developed a set of dc SQUIDs intended for frequency-domain multiplexed readout of Transition Edge Sensor (TES) arrays. The first design is based on the Ketchen-style washer, and has exhibited a $1.2 \times 10^{-7}\Phi_0$ Hz$^{1/2}$ flux noise both at 4.2 K and 0.43 K. The second design is based on the multiloop structure and utilizes the spoke-terminating resistors which double as junction shunts in order to minimize the excess noise due to the resonance damping. The multiloop device has exhibited a $3.5 \times 10^{-7}\Phi_0$ Hz$^{1/2}$ flux noise level at 4.2 K. The mutual inductances are chosen such that a typical ac-biased TES-based X-ray calorimeter would need only moderate amount of negative feedback in order to handle the dynamic range of the signal.

1. Introduction

Frequency-multiplexed readout of TESes can be performed by biasing a number of them with ac voltages [1] at different frequencies and reading out the summed current by a single SQUID [2]. Such a readout requires SQUIDs (i) capable of functioning at sub-kelvin temperatures, (ii) having a large natural dynamic range, and (iii) having a good energy resolution, i.e. simultaneously low current noise and low input inductance [3]. We describe design, fabrication and characterization of dc SQUIDs aimed for such a purpose.

2. Design

The dynamic range of the input current to a dc SQUID operating without negative feedback can be improved by reducing its flux noise

$$\Phi_n = \sqrt{2\epsilon L_{sq}} \tag{1}$$

simultaneously with reducing its mutual inductance between the input and the SQUID loop. L_{sq} is the loop inductance encountered by the Josephson junctions and the internal energy resolution can be expressed as [4]

$$\epsilon = 12k_BT\sqrt{L_{sq}Cj} + \hbar, \tag{2}$$

† Correspondence to Mikko.Kiviranta@vtt.fi

where the quantum limit has been qualitatively taken into account. One sees from (1) that it is advantageous to reduce L_{sq} as much as possible. Decrease of junction capacitance C_j has a smaller effect through (2), but it would also help matching to the room-temperature amplifier because the dynamic output resistance of a well-damped dc SQUID can be estimated as $R_d \approx (L_{sq}/2\pi C_j)^{1/2}$.

2.1. Washer SQUID

One SQUID type is based on the ordinary washer design. Crossing slits in two superconductive planes define the $L_{sq} \approx 7$ pH loop inductance and a 10-turn input coil leads to mutual inductance of $M^{-1} \approx 30$ μA/Φ_0. Large $dV/d\Phi_0$ is desirable in order to reduce the noise contribution due to the room-temperature amplifier; this, however, depends primarily on the trilayer properties. It can be shown that an order-of-magnitude value for a well-damped SQUID is $dV/d\Phi \approx \sqrt{J_c/\pi\Phi_0 C_D}$, where J_c is the critical current density and C_D is the capacitance density of the trilayer sheet.

There is an integrated 1:5 on-chip transformer at the SQUID output, boosting the output impedance level to 50 Ω for signals with f > 3 MHz. The junction shunting resistors are coupled to large-volume cooling fins in order to counteract the decoupling of the electron and phonon systems which takes place at sub-kelvin temperatures [5].

The resonances [4] [6] associated with such a short 10-turn input coil are at high frequencies; the microstrip length alone would set the $\lambda/2$-resonance at 25 GHz. Still, in frequency-domain multiplexers, it is difficult to obtain high loop gains in the flux-locked configuration, such that the applied flux (and subsequently the voltage, in a current-biased case) may vary significantly around the flux setpoint, and it may not be always possible to keep the Josephson frequency corresponding to the point of operation far from resonances. Thus the resonances of both the input coil and the output transformer need to be damped with proper RC shunts.

The optimal value of the microstrip-terminating resistance was determined from numerical simulations[7] involving a semi-distributed circuit model of the washer – input-coil combination, and it was found to be different from both the characteristic microstrip impedance and the characteristic impedance of the LC resonance‡. In practice two RC shunts with different R vales and different RC cutoff frequencies can be used as the termination.

2.2. Multiloop SQUID

Another approach to damp the resonances in the coupling circuitry is taken by a modification of the multiloop structure [9] [10] as depicted in fig. 1. The impedance seen between the ground and the driving point (e.g. **C** or **F** in fig.1) of a properly terminated transmission line is in theory resistive and frequency-independent. The parallel connection of n such impedances

‡ The lowest microstrip resonance degenerates into an LC resonance, in which also the loop-coupling inductance of the input coil and not only the stray inductance of the microstrip plays a role. Damping of microstrip resonances would require $R_s = \sqrt{L_s/C_s}$, whereas an LC-resonance would require $R_s = \sqrt{(n^2 L_{sq} + L_s)/C_s}$

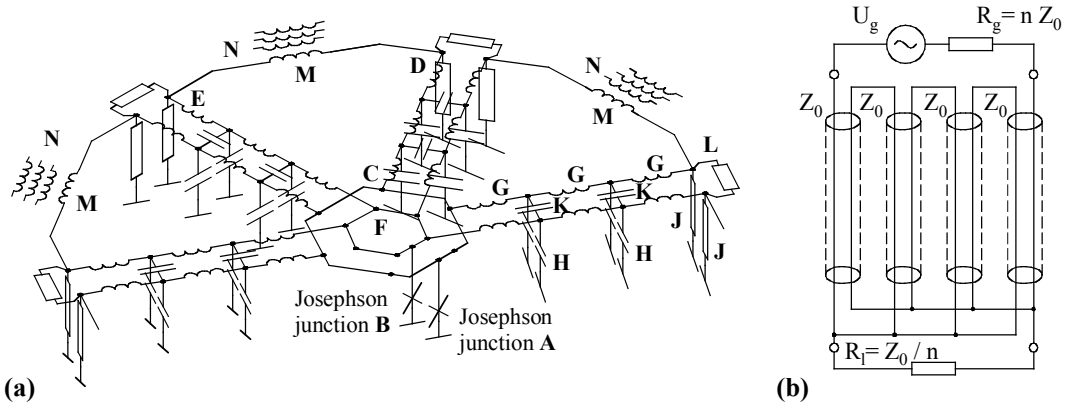

Figure 1. **(a)** Schematic structure of the multiloop SQUID. The loop inductance L_{sq} encountered between the top electrodes of the Josephson junctions **A** and **B** is formed by parallel connection of n subloops **C**→**D**→**E**→**F**. The distributed inductance **G** (of value L_s) together with the distributed capacitance **H** (of value C_s) present in the spokes form transmission lines which are terminated by resistors **J** of value $R_s = \sqrt{L_s/C_s}$. Interaction between the two transmission lines forming a spoke is depicted with the distributed capacitance **K**, and its effect to the characteristic impedance may be corrected for by the resistor **L**. The inductances **M** (of value L_p for the total circumference) couple to the turns of the input coil **N**. **(b)** A Guanella transformer, matching the generator impedance nZ_0 to the load impedance of Z_0/n with an aid of n transmission lines with characteristic impedance of Z_0.

can be used as junction shunting resistance, so that there will be no excess noise generators present due to resonance damping when the damping resistors double as junction shunts. Additionally, (i) smaller loop inductances can be realized than in the lithography-limited washer approach, and (ii) resistors are located far from the junctions where there is more room for the large resistor volume needed to overcome the poor electron-phonon coupling.

The loop inductance sensed by the J-junctions is $L_{sq} = L_p/n^2 + 2L_s/n$ (refer to fig.1) and the mutual inductance relating the current injected to the circumference to the flux effectively applied to the SQUID is $M = L_p/n$. One should take into account the condition that junctions with capacitance C_j must be non-hysteretic, i.e. $Z_0/n = \sqrt{L_{sq}/\pi C_j}$, where $Z_0 = \sqrt{L_s/C_s}$ is the characteristic impedance of the spoke transmission line. If one then expresses the spoke inductance $L_s = aZ_0/v_p$ in terms of the loop radius a and the signal propagation speed § v_p, and uses the formula $L_p = \xi\mu_0 a$ for the circumferic inductance where slowly varying prefactors are lumped into $\xi \approx 5$, one finds that the standard equation for the coupled energy sensitivity (2) of the device is modified into

$$\epsilon_c = \frac{1}{2}L_{in}i_n^2 = 12k_BT\left(\frac{1}{n}\sqrt{L_pC_j} + \frac{2L_p}{\sqrt{\pi}\xi\mu_0 v_p}\right). \qquad (3)$$

because of degradation of the coupling constant. Here i_n is the noise-equivalent input current and L_{in} the input inductance. Note that there is an n-independent penalty term, which is the price paid for the transformation of the inductance level from L_{sq} into L_p. We suspect that a similar penalty is present in every transformation scheme, another example being described in

§ Depends primarily on the permittivity of the insulator by $v_p = c/\sqrt{\epsilon_{r,eff}}$, where c is the vacuum speed of light.

[11]. The penalty prevents one from obtaining an arbitrarily good energy resolution by simply increasing the number of subloops n.

In practice the device optimization must be performed numerically, due to the presence of kinetic inductance in the superconducting lines, the interaction of nearby lines, evoking modes other than (quasi-) TEM at high frequencies and a number of other factors.

The device described here has 32 subloops and 190 μm loop radius, circumscribed by a 3-turn input coil. The resulting loop inductance is $L_{sq} \approx 1.0$ pH and the mutual inductance is approximately 30 μA / Φ_0. A fabricated device is shown in fig. 3.

Note that if one of the coupling inductances **M** was cut and input current fed to the exposed wire ends, the multiloop structure depicted in fig.1(a) would function effectively like a Guanella transformer [12] depicted schematically in fig.1(b).

3. Processing

The device fabrication consists of the following steps. First a 150/7/32 nm Nb/Al-AlOx/Nb trilayer with the critical current density of $J_c = 1.2 \times 10^7$ A/m^2 is deposited in situ on 100 mm diameter Si wafers. The top Nb is then removed everywhere else but at the intended locations of J-junctions, in order to avoid formation of parasitic J-junctions in contact windows. Junction areas are patterned by anodization to 60 volts, and the first superconductive wiring layer is patterned from the trilayer.

Next, a CMP-planarized‖, 250 nm thick PECVD SiO_2 layer is deposited. On top of this, a 2/65/2 nm Ti/Pd/Ti resistor layer is deposited by e-beam evaporation, and patterned by lift-off. A subsequent 100 nm SiO_2 layer is deposited before buffered hydrofluoric acid (BHF) wet etch of the contact windows. The BHF etches through the top half of SiO_2 and stops at the Pd in regions where the resistive layer is present, but etches through both halves and stops at the Nb/AlOx/Nb trilayer where Pd is not present. This trick to save one lithographic step is similar to the one used in the Berkeley process [8].

On top of the first insulator, the second superconductive Nb layer is sputtered after a short in-situ ion milling step whose purpose is to clean away the Nb and Ti native oxides present in the contact windows. The Nb is patterned with CF_4 + O_2 RIE, and covered with the second PECVD SiO_2 insulator. Contact windows are then etched with CHF_3 + O_2 RIE after a CMP planarization step. Finally the third Nb wiring layer is deposited and RIE patterned, and Al deposited as the bondable metal to the bonding pads. The presence of O_2 in the RIE plasma leads to a controlled resist erosion, which results in smoother film edges and better step coverage.

The resulting thin film stack is depicted in Fig. 2. The fabrication process has evolved from the standard VTT process [13].

‖ Chemical-Mechanical Polishing

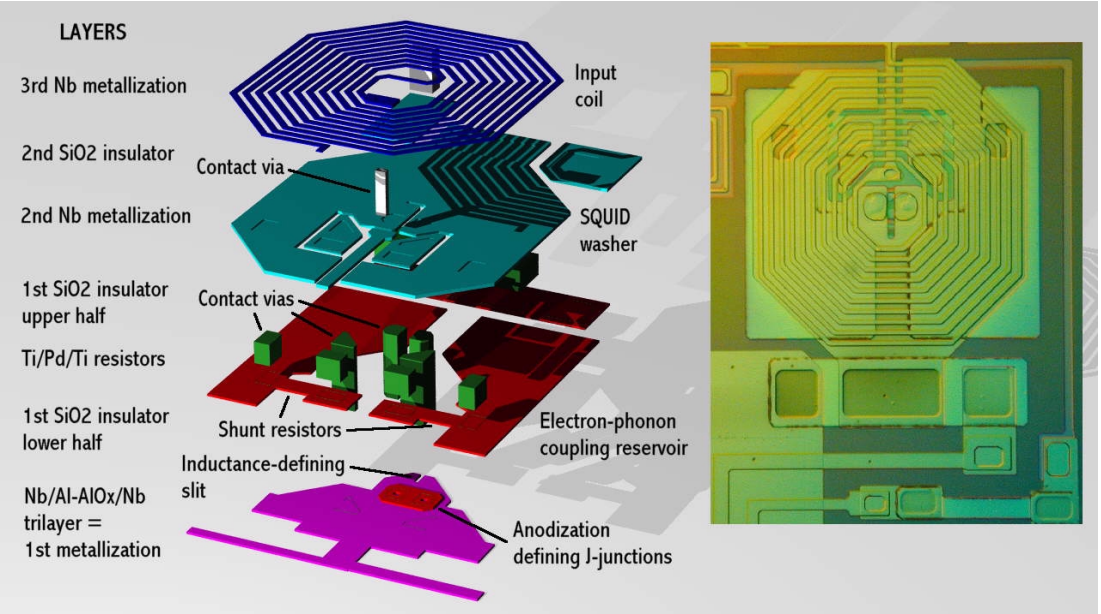

Figure 2. Exploded view of the layer stucture forming the washer SQUID. A microphotograph of a processed washer is shown in the inset.

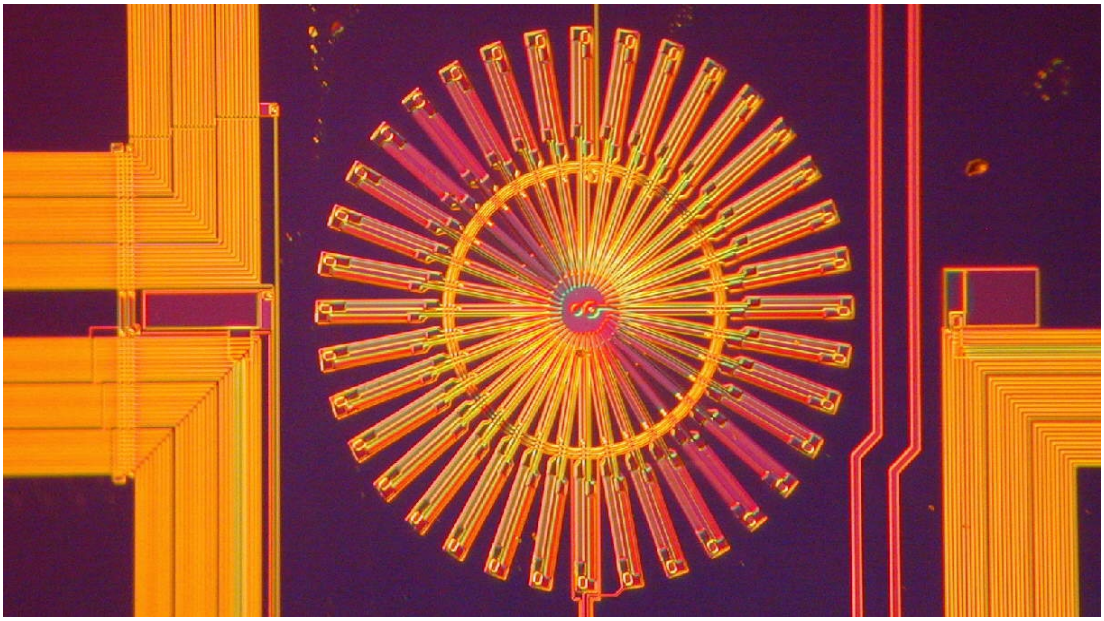

Figure 3. A microphotograph of a multiloop SQUID.

4. Measurements

The measurement setup consists of a preamplifier SQUID with a direct readout by an operational amplifier. The preamplifier SQUID is operated in a flux-locked loop through a simple 300 kHz-bandwidth controller. The preamplifier SQUIDs have been processed in the same fabrication run as the Devices Under Test (DUTs): they are versions of the washer SQUID equipped with an on-chip intermediate transformer boosting the mutual inductance to

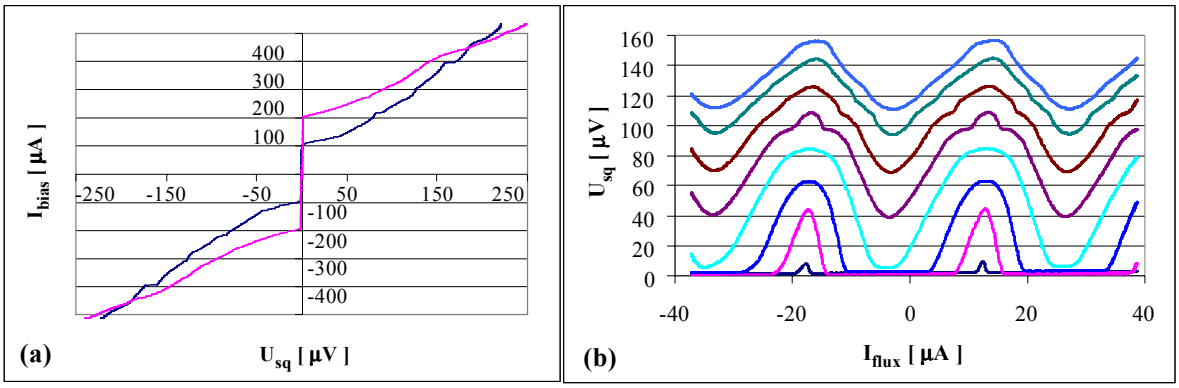

Figure 4. (a) Current-to-voltage characteristics of the washer SQUID at applied flux of approximately $n\Phi_0$ and $(n + \frac{1}{2})\Phi_0$. (b) Flux-to-voltage characteristics at bias currents I_b of approximately 110, 140, 170, 200, 240, 270, 310 and 330 μA

.

$M^{-1} = 2.5\mu\text{A}/\Phi_0$.

The DUT is current biased and its voltage is fed to the input coil of the preamplifier SQUID through a 3.3 Ω resistor. The DUT is operated in open loop, i.e. without flux feedback, and its gain $dV/d\Phi$ at the operating point is measured by applying a small test flux of about 1/50 Φ_0 amplitude prior to and after the noise measurement. The measurements were performed with a 4.2 K dipstick, and with a CEA Grenoble ^{3}He sorption cooler installed in an Infrared Laboratories' dewar.

4.1. Washer SQUID

The washer SQUID characteristics are shown in fig.4. The measured white flux noise of 0.12 $\mu\Phi_0\text{Hz}^{-1/2}$ (fig.5) corresponds to energy resolution of 42$\hbar$. Approximately the same flux noise level was measured both at 4.2 K and 430 mK temperature, which suggests that an excess noise mechanism is present, possibly due to the room-temperature bias circuitry. The origin of the excess noise at low frequencies is likely to be the dissipative currents flowing in the copper tape used ot attach the SQUID to the cold finger of the cryostat. Investigations to find the mechanisms are underway.

4.2. Multiloop SQUID

The multiloop SQUID characteristics are shown in fig.6. The structure present in characteristics suggests that the termination of the transmission lines is less-than-perfect. Regardless of the presence of resonances we have measured 0.35 $\mu\Phi_0\text{Hz}^{-1/2}$ white noise level (Fig. 7).

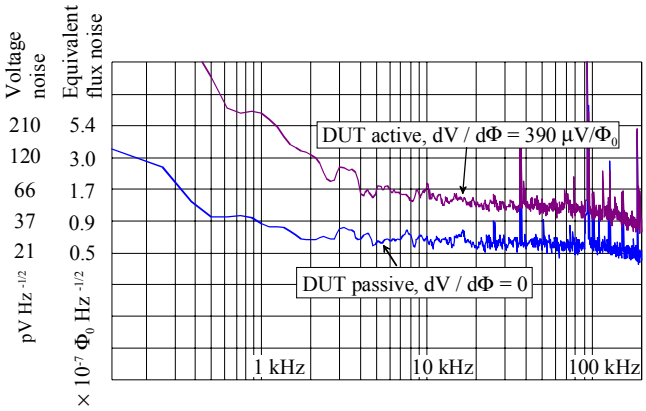

Figure 5. The measured voltage noise ($T = 0.43$ K) at the washer SQUID output and the equivalent flux noise. The contribution of readout circuitry is estimated by measuring the noise at the zero-gain point of operation.

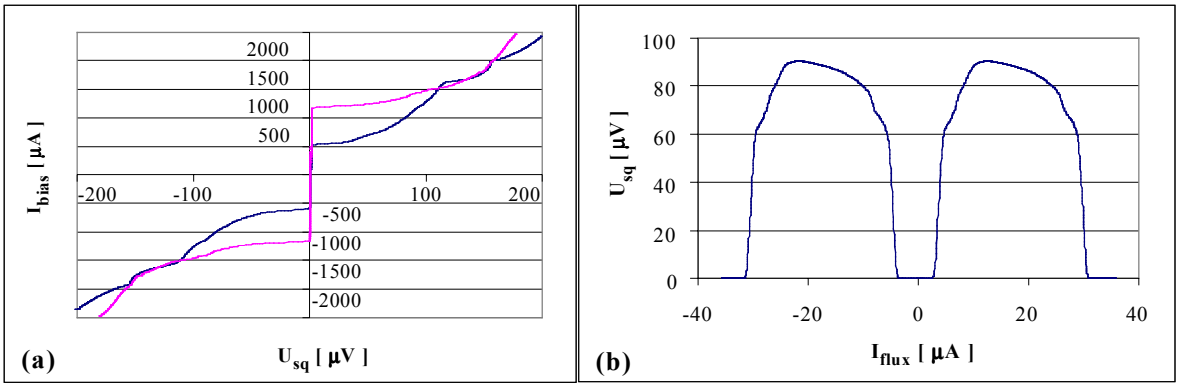

Figure 6. (a) Current-to-voltage characteristics of the multiloop SQUID at applied flux of approximately $n\Phi_0$ and $(n+\frac{1}{2})\Phi_0$. (b) Flux-to-voltage characteristics at the 1 mA bias current used in the noise measurement.

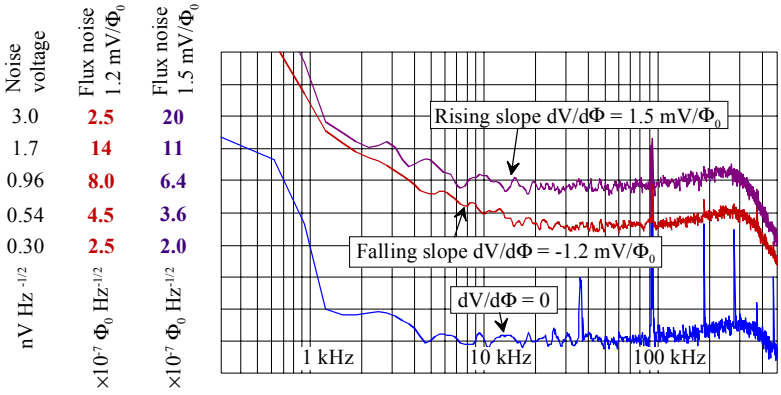

Figure 7. The measured voltage noise at the output of the multiloop SQUID, measured at $T = 4.2$ K on the rising slope, falling slope and zero-gain point of the flux-to-voltage characteristics. The voltage noise is scaled by the measured $dV/d\Phi$ to obtain flux noise.

5. Conclusion

We have succesfully fabricated two SQUID types which can be used in multiplexed TES readout. The devices have been tested down to 0.43 K temperature. Their noise-equivalent input currents of 3.6 pA $\mathrm{Hz}^{-1/2}$ and 11 pA $\mathrm{Hz}^{-1/2}$ are below the noise floor of the intended TES type [1], and they can handle the typical current swing of about 200 $\mu\mathrm{A}_{p-p}$ of an ac-biased TES when negative feedback with loop gain of about 7 (even though more is needed for linearization) is used. The low noise current of the washer device would even allow further increase of maximum current by reduction of numbers of turns in the input coil. It is conceivable that the flux noises can be improved over the figures described here by improving the room-temperature biasing circuitry in the case of the washer SQUID, and by more careful termination of the spoke striplines in the case of the multiloop SQUID.

Acknowledgments

We would like to thank the Space Research Organization of the Netherlands for lending the ^{3}He sorption cooler. This work has been partially funded from the Antares program of the National Technology Agency of Finland TEKES.

References

[1] van der Kuur J, de Korte P A J, Hoevers H F C, Kiviranta M and Seppä H 2002 *Appl. Phys. Lett.* **81** (23) pp 4467–9
[2] Kiviranta M, Seppä H, van der Kuur J, de Korte P 2002 *Proc. 9th Int. Workshop on Low Temperature Detectors (Madison)*, Porter F S, McCammon D, Galeazzi M and Stahle C, eds., (Melville: American Institute of Physics) pp 295–300
[3] Kiviranta M, Penttilä J S, Grönberg L, Seppä H and Suni I 2003 *IEEE Tran. Appl. Supercond.* **13** (2) pp 614–7
[4] Ryhänen T, Seppä H, Ilmoniemi R and Knuutila J 1989 *J. Low Temp. Phys.* **76** (5/6) p 330
[5] Wellstood F C 1989 *IEEE Tran. Magn.* **25** (2) pp 1001–4
[6] K. Enpuku, R. Cantor and H. Koch 1992 *J. Appl. Phys* **72** (3) pp 1000–6
[7] J. S. Penttilä and M. Kiviranta, unpublished.
[8] Meng X, Bhat A and van Duzer T, 1999 *IEEE Tran. Appl. Supercond.* **9** (2) pp 3208–11
[9] Zimmerman J E 1971 *J. Appl. Phys.* **42** (11) pp 4483–7
[10] Drung D, Knappe S and Koch H 1995, *J. Appl. Phys.* **77** (8) pp 4088–98
[11] Seppä H and Kiviranta M 1999 *Extended Abstracts of 7th International Superconductive Electronics Conference (Berkeley)* pp 155–7
[12] Sevick J 1996 *Transmission Line Transformers* (Atlanta: Noble Publishing) chapter 8
[13] H. Seppä et al 1993, *IEEE Tran. Appl. Supercond.* **3** (1) pp 1816–9